Published online 2 May 2017

Nucleic Acids Research, 2017, Vol. 45, No. 12 ***7401–7415***
doi: 10.1093/nar/gkx354

ALKBH1 is an RNA dioxygenase responsible for cytoplasmic and mitochondrial tRNA modifications

Layla Kawarada, Takeo Suzuki, Takayuki Ohira, Shoji Hirata, Kenjyo Miyauchi and Tsutomu Suzuki*

Department of Chemistry and Biotechnology, Graduate School of Engineering, University of Tokyo, 7-3-1 Hongo, Bunkyo-ku, Tokyo 113-8656, Japan

Received March 29, 2017; Revised April 17, 2017; Editorial Decision April 18, 2017; Accepted April 22, 2017

ABSTRACT

ALKBH1 is a 2-oxoglutarate- and Fe^{2+}-dependent dioxygenase responsible for multiple cellular functions. Here, we show that ALKBH1 is involved in biogenesis of 5-hydroxymethyl-2′-*O*-methylcytidine (hm^5Cm) and 5-formyl-2′-*O*-methylcytidine (f^5Cm) at the first position (position 34) of anticodon in cytoplasmic $tRNA^{Leu}$, as well as f^5C at the same position in mitochondrial $tRNA^{Met}$. Because f^5C34 of mitochondrial $tRNA^{Met}$ is essential for translation of AUA, a non-universal codon in mammalian mitochondria, *ALKBH1*-knockout cells exhibited a strong reduction in mitochondrial translation and reduced respiratory complex activities, indicating that f^5C34 formation mediated by ALKBH1 is required for efficient mitochondrial functions. We reconstituted formation of f^5C34 on mitochondrial $tRNA^{Met}$ *in vitro*, and found that ALKBH1 first hydroxylated m^5C34 to form hm^5C34, and then oxidized hm^5C34 to form f^5C34. Moreover, we found that the frequency of 1-methyladenosine (m^1A) in two mitochondrial tRNAs increased in *ALKBH1*-knockout cells, indicating that ALKBH1 also has demethylation activity toward m^1A in mt-tRNAs. Based on these results, we conclude that nuclear and mitochondrial ALKBH1 play distinct roles in tRNA modification.

INTRODUCTION

Cellular RNAs contain numerous chemical modifications that are introduced enzymatically after transcription. More than 130 types of modified nucleosides have been reported in various RNA molecules from all domains of life (1), of which about 80% of them were found in tRNAs. tRNA modifications ensure proper tRNA function of tRNAs by stabilizing tertiary structure, and fine-tuning decoding properties for translation (2). A wide variety of RNA modifications are present at the first position (wobble position or position 34) of tRNA anticodons. These modifications play pivotal roles in accurate and efficient translation by modulating codon–anticodon interaction at the ribosomal A-site (3).

5-Formylcytidine (f^5C) (Figure 1A), first discovered in mammalian mitochondrial (mt) tRNA (Figure 1B) (4), is a unique modification found at position 34 of mt-$tRNAs^{Met}$ from vertebrates and nematodes (4–6). In mammalian mitochondria, the AUA codon specifies Met instead of Ile (7). *In vitro* translation revealed that f^5C34 enables mt-$tRNA^{Met}$ to recognize AUA as well as AUG (8). Because the sole mt-$tRNA^{Met}$ acts in both initiation and elongation in mitochondrial protein synthesis, f^5C34 is an essential modification for mitochondrial protein synthesis. A structural study of the codon–anticodon interaction at the ribosomal A-site revealed that f^5C34 pairs with adenosine at the third letter of the AUA codon in a canonical Watson–Crick geometry, implying that f^5C undergoes imino-oxo tautomerization to pair with AUA (9). Since the discovery of this modification, however, biogenesis and physiological role of f^5C34 remained unresolved. Last year, we demonstrated that biogenesis of f^5C34 is initiated by *S*-adenosylmethionine (AdoMet)-dependent methylation catalyzed by NSUN3 (6). Knockout (KO) of *NSUN3* resulted in severe reduction in mitochondrial protein synthesis and respiratory activity, leading to mitochondrial dysfunction. We successfully reconstituted formation of 5-methylcytidine (m^5C) at the wobble position of mt-$tRNA^{Met}$ with recombinant NSUN3 in the presence of AdoMet, suggesting that f^5C34 is synthesized by NSUN3-mediated m^5C34 formation, followed by hydroxylation and oxidation of the methyl group.

We identified two pathogenic point mutations (A4435G and C4437U) in mt-$tRNA^{Met}$ (Figure 1B) that impaired m^5C34 formation by NSUN3 (6). These mutations are associated with mitochondrial diseases presenting with maternally inherited hypertension, Leber's hereditary optic neuropathy, hypotonia, seizure, muscle weakness, lactic acidosis and hearing loss (10–12). In addition, a loss-of-function mutation in *NSUN3* was identified in a patient presenting with symptoms of mitochondrial disorder, including devel-

*To whom correspondence should be addressed. Tel: +81 3 5841 8752; Fax: +81 3 5841 0550; Email: ts@chembio.t.u-tokyo.ac.jp

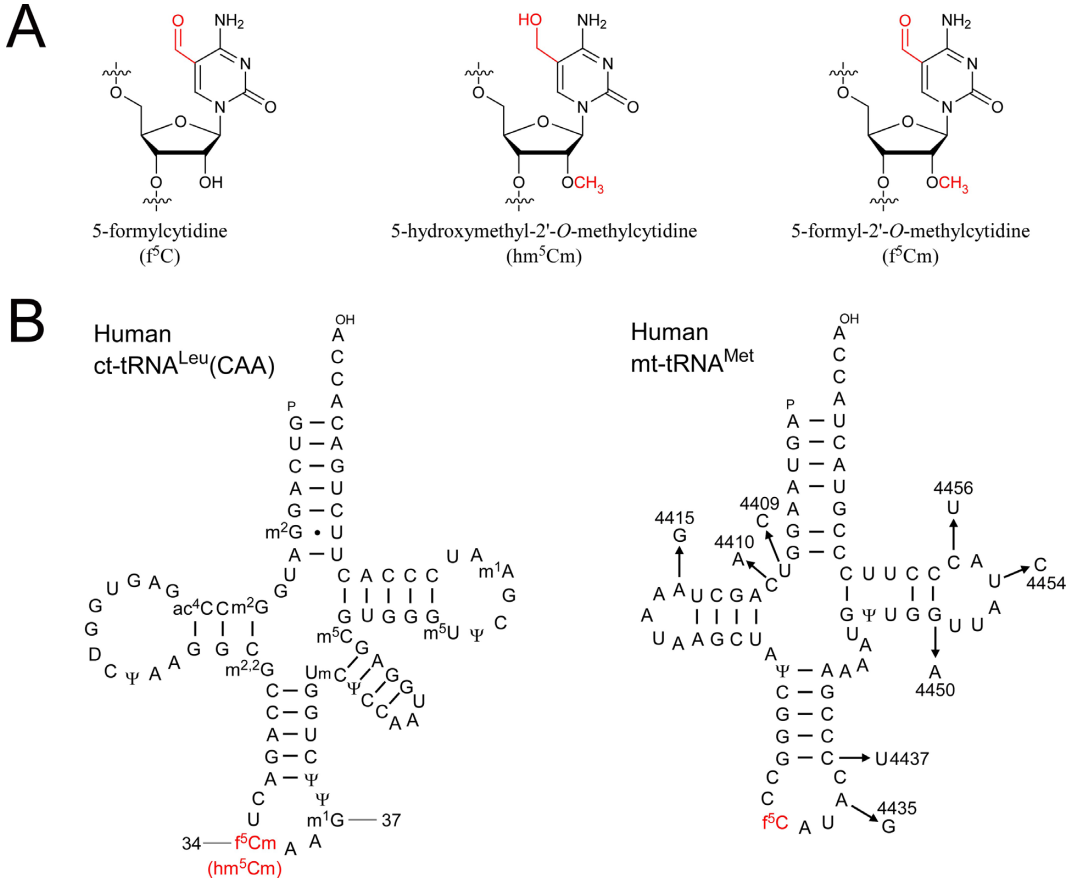

Figure 1. 5-Formylcytidine (f^5C) and derivatives found in human tRNAs. (**A**) Chemical structures of 5-formylcytidine (f^5C), 5- hydroxymethyl-2′-*O*-methylcytidine (hm^5Cm) and 5-formyl-2′-*O*-methylcytidine (f^5Cm). Modified groups are shown in red. (**B**) Secondary structures of human ct-$tRNA^{Leu}$(CAA) (left) and mt-$tRNA^{Met}$ (right) with post-transcriptional modifications: 2-methylguanosine (m^2G), N^4-acetylcytidine (ac^4C), dihydrouridine (D), pseudouridine (Ψ), 2,2-dimethylguanosine ($m^{2,2}G$), 1-methylguanosine (m^1G), 2′-*O*-methyluridine (Um), 5-methylcytidine (m^5C), 5-methyluridine (m^5U) and 1-methyladenosine (m^1A). f^5C and derivatives are shown in red. Modified positions are numbered as previously described (41,67). Eight pathogenic point mutations are indicated in human mt-$tRNA^{Met}$.

opmental disability, microcephaly, muscular weakness, external ophthalmoplegia and lactic acidosis (13,14). These observations indicated that loss of f^5C34 or *NSUN3* results in pathological consequence.

In a previous study, ALKBH1 could oxidize m^5C34 in the anticodon-stem loop of mt-$tRNA^{Met}$ to form f^5C34 *in vitro* (15), although hm^5C34 was not detected. Indirect detection of f^5C34 using chemical derivatization combined with primer extension revealed that the fraction of f^5C34-containing mt-$tRNA^{Met}$ decreased upon *ALKBH1* knockdown, indicating that ALKBH1 is involved in f^5C34 formation. However, hm^5C34 and m^5C34 could not be distinguished in this experiment, and it remained unclear to what extent ALKBH1 contributes to this process in the cell. Considering that ALKBH1 is involved in demethylation of N^6-methyldeoxyadenosine (m^6dA) in genomic DNA (16) and demethylation of 1-methyladenosine (m^1A) in cytoplasmic (ct-)tRNAs (17), it was necessary to perform a more sophisticated analysis of the modification status of tRNAs with the goal of obtaining direct evidence for ALKBH1 as an RNA oxygenase responsible for f^5C34 formation.

On the other hand, 2′-*O*-methyl derivative of f^5C (5-formyl-2′-O-methylcytidine, f^5Cm) (Figure 1A) is present at the wobble position of mammalian ct-$tRNA^{Leu}$ with the CAA anticodon (Figure 1B) (18). Given that f^5C allows tRNA to pair with A (8), this modification has been speculated to permit the recognition of UUA in addition to UUG. Notably, the 5-hydroxymethylcytidine derivative hm^5Cm (Figure 1A), a reduced form of f^5Cm, has also been detected in this tRNA (18), strongly indicating that f^5Cm and hm^5Cm are synthesized via oxidation of m^5C. A metabolic labeling study revealed that hm^5C and f^5C in mouse total RNA are generated by oxidation of m^5C (19), indicating that hm^5Cm and f^5Cm in ct-$tRNA^{Leu}$(CAA) are synthesized by hydroxylation and oxidation of m^5C. However, the RNA dioxygenase responsible for this process has not been previously identified.

Here, we report that ALKBH1 is an RNA dioxygenase involved in biogenesis of hm^5Cm34 and f^5Cm34 in ct-$tRNA^{Leu}$, as well as f^5C34 in mt-$tRNA^{Met}$, *ALKBH1*-knockout cells exhibited a strong reduction in mitochondrial translation and reduced oxygen consumption, indicating that ALKBH1 is required for efficient mitochondrial activity. We successfully reconstituted formation of hm^5C and f^5C with ALKBH1 in the presence of 2-oxoglutarate (2-OG) and Fe^{2+}, demonstrating that f^5C is synthesized by

consecutive hydroxylation and oxidation of m^5C. We also examined several pathogenic mutations in mt-$tRNA^{Met}$ associated with mitochondrial diseases, but these mutations had little effect on f^5C formation mediated by ALKBH1, indicating that these diseases are caused by lack of f^5C in the mutant tRNAs resulting from defective methylation by NSUN3, but not from defective oxidation by ALKBH1. Moreover, we found that the frequency of m^1A in two mt-tRNAs increased in *ALKBH1* KO cells, indicating that ALKBH1 also has demethylation activity toward m^1A in some mt-tRNAs.

MATERIALS AND METHODS

Cell culture and measurement of cell proliferation

HEK293T cells were cultured in high-glucose Dulbecco's modified Eagle's medium (DMEM) supplemented with 10% fetal bovine serum (FBS) and 1% penicillin–streptomycin at 37°C under a humidified atmosphere containing 5% CO_2. *ALKBH1* KO and *NSUN3* KO HEK293T cells were cultured in DMEM (high-glucose) supplemented with 10% FBS, 1% penicillin–streptomycin, 0.11 g/l sodium pyruvate and 0.05 g/l uridine. For measuring cell proliferation, wild-type (WT) and KO HEK293T cells were seeded on 96-well plates (8.0×10^3 cells per well) in glucose medium (no-glucose DMEM supplemented with 2 mg/ml glucose) or galactose medium (no-glucose DMEM supplemented with 2 mg/ml galactose) supplemented with alamarBlue reagent (Invitrogen). The plates were incubated at 37°C for 3 h, and the absorbances at 570 and 600 nm were measured on a SpectraMax 190 microplate reader (Molecular Devices). Cell proliferation was evaluated based on the percentage of reduced dye.

Construction of *ALKBH1* KO lines

The human *ALKBH1* gene was knocked out using the CRISPR-Cas9 system basically as described (20). We designed an sgRNA targeting exon 4 of *ALKBH1* gene. Sense and antisense DNAs for the sgRNA (Supplementary Table S1) were cloned into vector pX330 (Addgene plasmid 42230). HEK293T cells (2.0×10^5 cells per well) were transfected with the cloned vector (300 ng) and seeded on 24-well plates. The KO efficiency of each sgRNA was evaluated by surveyor assay using a specific pair of primers (Supplementary Table S1). The cells were diluted and sub-cultured on 10 cm dishes. Eleven days after the transfection, colonies were isolated and genomic DNAs were extracted. *ALKBH1* KO lines were selected by confirming the frameshift mutations in the target region.

RNA extraction and tRNA isolation

Total RNA was extracted from HEK293T cells using TriPure Isolation Reagent (Roche Life Science). Total RNA from mouse fetus was kindly provided by S. Nakagawa (Hokkaido University). Individual tRNAs were isolated by reciprocal circulating chromatography (RCC) (21,22) using the 5′-terminal ethylcarbamate amino-modified DNA probes listed in Supplementary Table S1.

RNA mass spectrometry

Isolated tRNA (1–2 pmol) was digested with RNase T_1, RNase A or MazF (Takara Bio.) at 37°C for 30 min in 20 mM NH_4OAc (pH 5.3), followed by mixing with an equal volume of 100 mM triethylamine–acetate and subjected to capillary liquid chromatography (LC)–nano–electrospray ionization (ESI)–mass spectrometry (MS) as described (22–24).

cDNA cloning and expression of recombinant ALKBH1

The cDNA of human ALKBH1 (GenBank NM_006020.2) was obtained by nested polymerase chain reaction from total RNA of HEK293T cells using specific primers (Supplementary Table S1) and cloned into pE-SUMO-NSUN3 (6) using the In-Fusion HD cloning kit (Clontech) to yield pE-SUMO-ALKBH1. *Escherichia coli* Rosetta2 (DE3) (Novagen) was transformed with pE-SUMO-ALKBH1 and cultured at 25°C. When the OD_{600} reached 0.4, 10 μM Isopropyl β-D-1-thiogalactopyranoside (IPTG) was added, and the culture was incubated at 16°C for an additional 24 h. The harvested cells were lysed by sonication in a buffer consisting of 20 mM Tris–HCl (pH 7.5), 0.5 M KCl, 1 mM dithiothreitol (DTT) and 0.5 mM phenylmethanesulfonyl fluoride (PMSF). Soluble protein was loaded onto a HisTrap HP column (GE Healthcare) on an AKTA Purifier 10 system (GE Healthcare) and separated with 0–500 mM gradient of imidazole. Fractions containing His6-SUMO-tagged human ALKBH1 were collected and dialyzed overnight in buffer consisting of 20 mM Tris–HCl (pH 7.5), 0.5 M KCl, 1 mM DTT and 10% glycerol. The His6-SUMO tag was cleaved by ubiquitin-like specific protease 1 (Ulp1) at 4°C overnight, and then removed by passing the sample through HisLink protein proliferation resin (Promega). The untagged protein was equilibrated with a buffer consisting of 50 mM Tris–HCl (pH 8.0), 50 mM NaCl and 7 mM 2-mercaptoethanol, and further purified by Mono Q anion exchange chromatography (HR 5/5, GE Healthcare) with a gradient of NaCl (50–1000 mM) using AKTA Purifier 10 system (GE Healthcare). The purified ALKBH1 was dialyzed against a buffer consisting of 50 mM Tris–HCl (pH 8.0), 100 mM NaCl and 7 mM 2-mercaptoethanol, followed by addition of glycerol to 30% f.c.

In vitro reconstitution of f^5C34 by recombinant ALKBH1

WT and mutant mt-$tRNAs^{Met}$ were prepared by *in vitro* transcription using T7 RNA polymerase, basically as described (25). Synthetic DNAs for templates are listed in Supplementary Table S1. Anticodon stem-loop with m^5C34 was chemically synthesized by GeneDesign Inc. The *in vitro* transcribed mt-$tRNA^{Met}$ was methylated by recombinant NSUN3 (6) at 37°C for 90 min in a reaction mixture consisting of 20 mM HEPES–KOH (pH 8.0), 5 mM $MgCl_2$, 100 mM KCl, 1 mM DTT, 2.8 μM mt-$tRNA^{Met}$ transcript, 2.8 μM NSUN3 and 640 μM AdoMet. tRNA containing m^5C34 was extracted with phenol:chloroform:isoamylalcohol (25:24:1, v/v/v) and collected by ethanol precipitation. *In vitro* reconstitution of f^5C34 was performed at 37°C for 90 min in a reaction

mixture containing 20 mM HEPES–KOH (pH 6.8), 5 mM $MgCl_2$, 50 mM KCl, 1 mM DTT, 4 mM ascorbic acid, 100 μM 2-OG, 80 μM $(NH_4)_2Fe(SO_4)_2{\cdot}6H_2O$, 0.5 μM mt-tRNA^{Met} with m^{5}C34 and 0.125 μM recombinant ALKBH1. For the series of mt-tRNA^{Met} mutants, incubation time was 15 min. The reaction was stopped by addition of an equal volume of phenol:chloroform:isoamylalcohol (25:24:1, v/v/v), and tRNAs were precipitated with ethanol. The tRNA was digested with RNase T_1 and subjected to LC/MS to analyze modification status. For *in vitro* reconstitution of f^{5}C34 from C34, the unmodified mt-tRNA^{Met} was incubated at 37°C in a reaction mixture consisting of 20 mM HEPES–KOH (pH 8.0), 5 mM $MgCl_2$, 50 mM KCl, 1 mM DTT, 230 μM AdoMet, 4 mM ascorbic acid, 100 μM 2-OG, 80 μM $(NH_4)_2Fe(SO_4)_2{\cdot}6H_2O$, 0.5 μM tRNA transcript, 0.5 μM NSUN3 and 0.125 μM ALKBH1. Aliquots were taken at the indicated times (Figure 6C) and subjected to LC/MS as described above.

Mitochondrial activities

HEK293T WT, *ALKBH1* KO and *NSUN3* KO cells (4.0×10^7) were suspended in 3 ml MOPS buffer consisting of 10 mM MOPS, 250 mM sucrose and 1 × Complete Mini Protease Inhibitor Cocktail Tablet (Roche), and then homogenized on ice by 12 up-and-down strokes with a Teflon homogenizer. The homogenate was centrifuged at 600 × *g* for 5 min at 4°C, and the supernatant was further centrifuged at 10 000 × *g* for 15 min at 4°C. The mitochondrial pellet was collected and resuspended in MOPS buffer. The activities of respiratory chain complexes were evaluated as described (26). The oxygen consumption rate (OCR) of WT, *ALKBH1* KO and *NSUN3* KO cells was measured using an XF24-3 extracellular flux analyzer (Seahorse Bioscience).

Pulse labeling of mitochondrial protein synthesis

HEK293T WT, *ALKBH1* KO and *NSUN3* KO cells (2.0×10^4) were seeded on 10 cm dishes and cultured overnight. Cells were washed with L-Met-, L-Gln- and L-Cys-free medium (Sigma-Aldrich) supplemented with 2 mM L-Gln, 10% FBS and 1 mM sodium pyruvate. To inhibit cytoplasmic protein synthesis, 50 μg/ml emetine was added to the medium and incubated for 10 min. The cells were further supplemented with 8.14 MBq (0.22 mCi) of [^{35}S] Met/[^{35}S] Cys (EXPRE^{35}S^{35}S Protein Labeling Mix, [^{35}S]-, PerkinElmer) and incubated for 1 h to label proteins translated in mitochondria. Then, the medium was replaced with cold medium (DMEM with 10% FBS) and chased for 10 min, and the cells were harvested by centrifugation at 1500 × *g* for 10 min at 4°C. The cell lysates were resolved by Tricine-sodium dodecylsulphate-polyacrylamide gel electrophoresis (SDS-PAGE) (16.5%), and the gel was coomassie brilliant blue (CBB)-stained and dried by a gel drier (AE-3750 RapiDry, ATTO). The dried gel was exposed to an imaging plate (BAS-MS2040, Fujifilm) and visualized on a FLA-7000 fluorimager (Fujifilm).

Primer extension to detect m^{1}A modification

Primer extension was conducted basically as described (27,28). The 5′ ^{32}P-labeled primer (0.1 pmol) was incubated with 3.125 μg total RNA in a 5 μl mixture containing 10 mM Tris–HCl (pH 8.0) and 1 mM EDTA for 2 min at 80°C, followed by cooling to room temperature. Subsequently, 0.5 μl (100 units) SuperScript III (Invitrogen) was added to 4.5 μl of the premixed solution [2 μl 5 × FS buffer (Invitrogen), 0.25 μl of 1.5 mM d/ddNTP mix, 0.75 μl ddH_2O and 1.5 μl of 25 mM $MgCl_2$]. The d/ddNTP mix consisted of dTTP, dGTP and ddCTP for mt-tRNA^{Lys}; dTTP, dGTP and ddATP for mt-tRNA^{Arg}; and dATP, dTTP, dCTP and ddGTP for mitochondrial 16S rRNA. The reaction was carried out for 1 h at 47°C for mt-tRNAs and 55°C for mitochondrial 16S rRNA. The reaction was stopped by addition of 0.5 μl of 4 M NaOH and boiling for 5 min at 95°C, and then neutralized by addition of 4.5 μl of 1 M Tris–HCl (pH 5.0). The cDNAs were resolved by 20% denaturing PAGE. The gel was exposed to an imaging plate (BAS-MS2040, Fujifilm) and visualized on a FLA-7000 fluorimager (Fujifilm).

RESULTS

Modification status of precursors and mature ct-tRNA^{Leu}(CAA)

In *Saccharomyces cerevisiae* and vertebrates, ct-tRNA^{Leu}(CAA) has an intron in its anticodon region (29,30), indicating that biogenesis of f^{5}Cm34 is coupled with intron removal via tRNA splicing. To study the biogenesis of f^{5}Cm34 in ct-tRNA^{Leu}(CAA), we first analyzed the modification status of their precursors by mass-spectrometric analysis (RNA-MS) and observed sequential formation of f^{5}Cm34. From mouse fetus, we isolated two precursors of ct-tRNA^{Leu}(CAA), along with its mature form by RCC (Figure 2A) (21). The isolated tRNAs were digested by RNase T_1 and subjected to RNA-MS to detect the anticodon-containing fragments (Figure 2B), which were then further probed by collision-induced dissociation (CID) to map the modified residues (Supplementary Figure S1). The primary transcript of ct-tRNA^{Leu}(CAA), bearing the 5′ leader, 3′ trailer and intron, mainly contained m^{5}C34. Only 1.2% of this precursor contained hm^{5}C34, and no f^{5}C34 was detected. On the other hand, the post-spliced precursor contained m^{5}C34 and hm^{5}C34 as major modifications, and f^{5}C34 was present in 6.9% of this precursor. In the mature ct-tRNA^{Leu}(CAA), hm^{5}C34m and f^{5}Cm34 were abundant. These results revealed the order and timing of each step of f^{5}Cm34 formation. Given that Trm4/NSUN2 methylates C34 in ct-tRNA^{Leu}(CAA) in an intron-dependent manner (31,32), m^{5}C34 must be introduced by NSUN2 in the primary transcript in the nucleus. After removal of the intron from the primary transcript, the post-spliced tRNA precursor undergoes hydroxylation and oxidation by an unknown enzyme to yield hm^{5}C34 and f^{5}C34. Followed by 5′ and 3′ processing and CCA addition, tRNA precursor is exported to the cytoplasm, where 2′-*O*-methylation takes place to yield hm^{5}Cm34 and f^{5}Cm34.

Biogenesis of hm^{5}Cm34 and f^{5}Cm34 in ct-tRNA^{Leu}(CAA)

According to our analyses of ct-tRNA^{Leu}(CAA), hydroxylation and oxidation of hm^{5}Cm34/f^{5}Cm34 must occur in

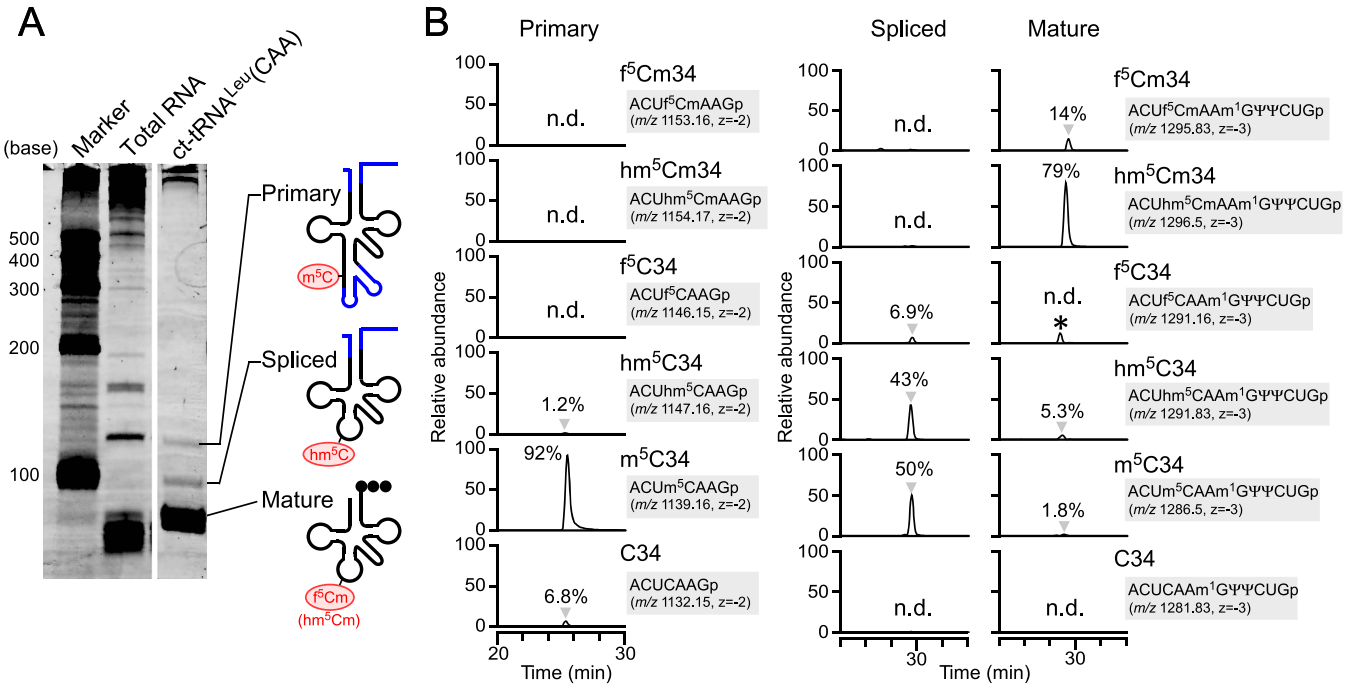

Figure 2. Modification status at the wobble position of precursor and mature ct-tRNA^{Leu} (CAA) (**A**) Isolation of ct-tRNA^{Leu}(CAA) from mouse fetus. Total RNA and isolated ct-tRNA^{Leu}(CAA) were resolved by electrophoresis on 10% polyacrylamide gels containing 7 M urea and stained with SYBR Gold. RNA bands for primary, spliced and mature tRNAs are indicated on the right. (**B**) Mass chromatograms of anticodon-containing fragments with f^{5}Cm34 (top), hm^{5}Cm34 (second), f^{5}C34 (third), hm^{5}C34 (forth), m^{5}C34 (fifth) and C34 (bottom) from primary (left), spliced (center) and mature (right) forms of ct-tRNA^{Leu}(CAA). The sequence of each fragment with *m/z* value and charge state is indicated. Frequency (%) of fragment with each modification is indicated. n.d., not detected. Gray triangles indicate target peaks, while asterisk indicates an unidentified fragment whose molecular mass differs from that of the target fragment. The 7-mer-fragments (positions 31−37) were detected in the primary tRNA, as G37 remained unmodified, whereas the 12-mer-fragments (positions 31−42) were detected due to the presence of m^{1}G37 in the spliced and mature tRNAs.

the nucleus because the post-spliced precursor that had not yet undergone end-maturation already contained hm^{5}C34 and f^{5}C34 (Figure 2B). We chose ALKBH1 as a candidate for the RNA dioxygenase responsible for this process based on its previously reported nuclear functions (16,33). We knocked out this gene in HEK293T cells using the CRISPR-Cas9 system and obtained two KO cell lines in which both alleles contained frameshift mutations (Figure 3A). Next, we isolated ct-tRNA^{Leu}(CAA) from *ALKBH1* KO cells and subjected it to RNA-MS to analyze its modification status (Figure 3B). In WT HEK293T cells, f^{5}Cm34 and hm^{5}Cm34 were abundantly detected in ct-tRNA^{Leu}(CAA). In *ALKBH1* KO cells, neither f^{5}Cm34 nor hm^{5}Cm34 were present, and instead m^{5}Cm34 was found, demonstrating that *ALKBH1* is responsible for conversion from m^{5}Cm34 to f^{5}Cm34/hm^{5}Cm34. Next, we selected FTSJ1 as a strong candidate for the tRNA methyltransferase responsible for 2′-*O*-methylation of f^{5}Cm34/hm^{5}Cm34, because FTSJ1 is localized in the cytoplasm and is involved in 2′-*O*-methylation of residues at positions 32 and 34 in the anticodon region (34,35). We knocked out this gene and obtained a *FTSJ1* KO cell line (Figure 3C). Ct-tRNA^{Leu}(CAA) was isolated from the KO cells and subjected to RNA-MS. As expected, both the f^{5}Cm34 and hm^{5}Cm34 detected in WT cells disappeared, and f^{5}C34 and hm^{5}C34 increased, in *FTSJ1* KO cells (Figure 3D), demonstrating that FTSJ1 is responsible for 2′-*O*-methylation of f^{5}Cm34/hm^{5}Cm34. According to yeast studies (36), Trm7p, an *S. cerevisiae* homolog of FTSJ1, introduces 2′-*O*-methylation at positions 32 and 34. To select different positions for methylation, FTSJ1 chooses two kinds of partner proteins, Trm732p and Trm734p, for positions 32 and 34, respectively. In human, as WDR6 is an apparent homolog of Trm734p, FTSJ1 complexed with WDR6 is likely to be involved in this process (Figure 3E).

Taken together, these results elucidate the biogenesis of hm^{5}Cm34 and f^{5}Cm34 in ct-tRNA^{Leu}(CAA) (Figure 3E). First, NSUN2 methylates C34 to give m^{5}C34 in the primary transcript of ct-tRNA^{Leu}(CAA) in the nucleus (32), followed by tRNA splicing to remove the intron in the anticodon loop. Then, m^{5}C34 in the post-spliced tRNA precursor is partially hydroxylated to form hm^{5}C34 and further oxidized to form f^{5}C34. During this process, the 5′ leader and 3′ trailer of the precursor are removed to become an end-matured precursor, which is then exported to the cytoplasm, where the wobble bases are 2′-*O*-methylated by FTSJ1 together with a partner protein (probably WDR6) to form hm^{5}Cm34 and f^{5}Cm34. On the other hand, in *ALKBH1* KO cells, ct-tRNA^{Leu}(CAA) containing m^{5}C34 is exported to the cytoplasm and methylated by FTSJ1 to form m^{5}Cm34.

Biogenesis of f^{5}C34 in mt-tRNA^{Met}

ALKBH1 is also localized in mitochondria (37). Hence, we investigated whether ALKBH1 is involved in f^{5}C formation of mt-tRNA^{Met}. For this purpose, we isolated mt-tRNA^{Met}

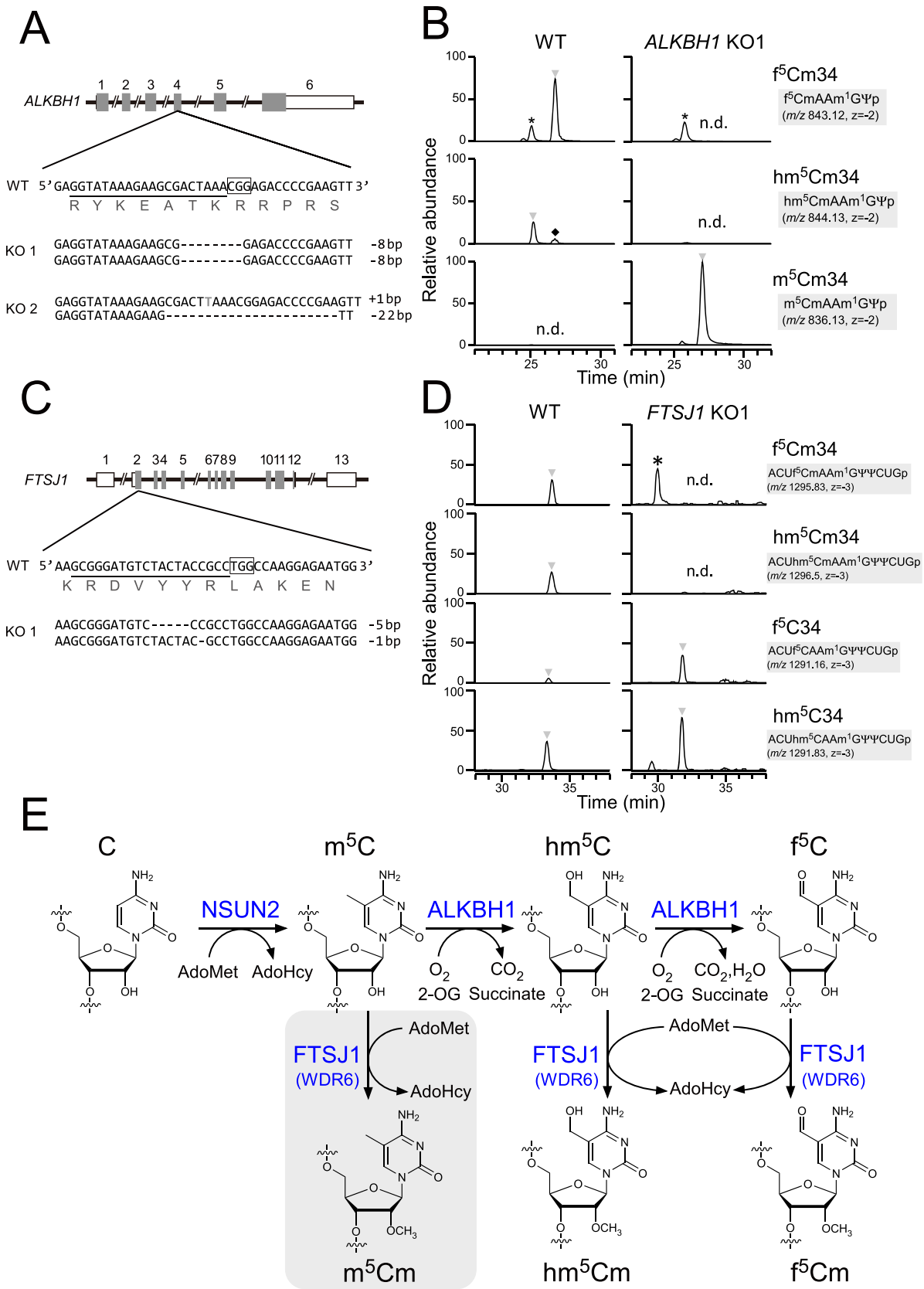

Figure 3. Genetic analyses of hm^{5}Cm34/f^{5}Cm34 formation in ct-tRNA^{Leu}(CAA) (**A**) Schematic depiction of the human *ALKBH1* gene and target site of mutations introduced by the CRISPR–Cas9 system. Shaded and open boxes indicate coding regions and untranslated regions of exons, respectively. Lines

from WT HEK293T cells and the *ALKBH1* KO cells, and analyzed the wobble modification by RNA-MS. As shown in Figure 4A, f^5C34 was fully introduced in mt-$tRNA^{Met}$ isolated from WT cells, whereas no hm^5C34, m^5C34 or C34 was clearly present. On the other hand, f^5C34 was completely absent, whereas m^5C34 was clearly present, in mt-$tRNA^{Met}$ isolated from *ALKBH1* KO cells, demonstrating that ALKBH1 is responsible for conversion from m^5C34 to f^5C34 in mt-$tRNA^{Met}$, and that no other enzymes are redundantly involved in this process. To confirm this result, we introduced plasmid-encoded *ALKBH1* into KO cells to rescue f^5C34 formation. RNA-MS analysis of the isolated mt-$tRNA^{Met}$ revealed that f^5C34 was restored (Figure 4A), albeit partially, probably due to inefficient transfection.

Based on these findings, we propose a reaction scheme for biogenesis of f^5C34 in mt-$tRNA^{Met}$ (Figure 4B). In this pathway, NSUN3 initiates formation of f^5C34 in mt-$tRNA^{Met}$ by AdoMet-dependent methylation of C34 to form m^5C34. Then, ALKBH1 hydroxylates m^5C34 to form hm^5C34, followed by oxidation of hm^5C34 to yield f^5C34.

Deletion of *ALKBH1* causes mitochondrial dysfunction

Because loss of f^5C in *NSUN3* KO cells results in mitochondrial dysfunction (6), we next examined the growth properties of *ALKBH1* KO cells in glucose and galactose media (Figure 5A). Mitochondrial activity is required for growth in a medium containing galactose as the primary carbon source (38). *ALKBH1* KO cells grew as well as *NSUN3* KO cells in glucose medium, but a bit slower than WT cells. Compared to WT cells, *ALKBH1* KO cells grew much more slowly in galactose medium, as also observed for *NSUN3* KO cells, indicating that *ALKBH1* is required for efficient mitochondrial activity. Next, we biochemically compared respiratory complex activities between *ALKBH1* KO, *NSUN3* KO and WT cells (Figure 5B). We observed a clear reduction of Complex I activity in *ALKBH1* KO and *NSUN3* KO cells, but no significant changes in the other complexes. The OCRs of *ALKBH1* KO and *NSUN3* KO cells were substantially lower than that of WT cells (Figure 5C), indicating that oxidative phosphorylation and respiratory activity of mitochondria were impaired by *ALKBH1* KO.

To examine mitochondrial protein synthesis, we conducted a pulse-labeling experiment in *ALKBH1* KO and *NSUN3* KO cells (Figure 5D). In cells treated with emetine to inhibit cytoplasmic translation, mitochondrial translation was specifically labeled by addition of [^{35}S] Met and [^{35}S] Cys for short periods of time. We found that mitochondrial protein synthesis was substantially reduced in *ALKBH1* KO and *NSUN3* KO cells in comparison to WT cells. This finding suggests that m^5C34 in mt-$tRNA^{Met}$ in *ALKBH1* KO cells cannot efficiently decipher the AUA codon.

In vitro reconstitution of f^5C modification

To examine the enzymatic activity of ALKBH1 responsible for f^5C formation, we performed *in vitro* reconstitution of f^5C34 in mt-$tRNA^{Met}$. For this purpose, *in vitro* transcribed mt-$tRNA^{Met}$ containing m^5C34 introduced by NSUN3 was incubated with recombinant ALKBH1 in the presence or absence of 2-OG and Fe^{2+}. The products were digested with RNase T_1 and subjected to RNA-MS (Figure 6A). We detected an f^5C34-containing fragment, along with a hm^5C34-containing fragment, only in the presence of both 2-OG and Fe^{2+}. These modified fragments were further probed by CID to confirm the presence of hm^5C and f^5C at position 34 (Figure 6B). In addition, we used the m^5C34-containing anticodon stem-loop (ASL) as a substrate (Figure 6A) and found that f^5C34 and hm^5C34 were clearly formed in this substrate. We also performed *in vitro* formation of f^5C34 from C34 via consecutive reactions mediated by NSUN3 and ALKBH1 (Figure 6C). In this experiment, unmodified mt-$tRNA^{Met}$ was incubated with NSUN3 and ALKBH1 in the presence of AdoMet, 2-OG and Fe^{2+}. During accumulation of m^5C34, hm^5C34 and f^5C34 gradually formed. Ultimately, 95% of tRNAs were methylated by NSUN3 after 2 h. Among the products, 74% contained hm^5C34, while 23% had f^5C34. This finding demonstrated that f^5C34 can be reconstituted by cooperative modifications with NSUN3 and ALKBH1.

These results suggest that ALKBH1 is a 2-OG- and Fe^{2+}-dependent RNA dioxygenase that hydroxylates and oxidizes m^5C34 to form hm^5C34 and f^5C34, respectively. Because ASL could be a substrate for f^5C34/hm^5C34 formation, ALKBH1 recognizes the anticodon–stem–loop region and does not require the entire tRNA structure for this reaction.

indicate introns. The target sequence of sgRNA in exon 4 is underlined, and the proto-spacer adjacent motif (PAM) sequence is boxed. Sequences of both alleles in KO1 and KO2 cell lines are aligned. Deleted nucleotides are indicated as dashed lines, and the inserted nucleotide is indicated by a gray letter. (**B**) Mass chromatograms of the anticodon-containing fragments of ct-$tRNA^{Leu}$(CAA) containing f^5Cm34 (top), hm^5Cm34 (middle) and m^5Cm34 (bottom) isolated from WT (left) and *ALKBH1* KO (right) cell lines. n.d., not detected. Target peaks are indicated by gray triangles. Filled diamond in the left middle panel indicates a trace of an isotopic ion of f^5Cm-containing fragment. Asterisk indicates an unidentified fragment whose molecular mass differs from that of the target fragment. (**C**) Schematic depiction of the human *FTSJ1* gene and target site of the mutation introduced by the CRISPR–Cas9 system. Shaded and open boxes indicate coding regions and untranslated regions of exons, respectively. Lines indicate introns. The target sequence of sgRNA in exon 2 is underlined, and the PAM sequence is boxed. Sequences of both alleles in KO1 cell lines are aligned. Deleted nucleotides are indicated by dashed lines. (**D**) Mass chromatograms of the anticodon-containing fragments of ct-$tRNA^{Leu}$(CAA) having f^5Cm34 (top), hm^5Cm34 (second), f^5C34 (third) and hm^5C34 (bottom) isolated from WT (left) and *FTSJ1* KO (right) cell lines. n.d., not detected. Target peaks are indicated by gray triangles. Filled diamond in the left second panel indicates a trace isotopic ion of the f^5Cm-containing fragment. Asterisk indicates an unidentified fragment whose molecular mass differs from that of the target fragment. (**E**) Biosynthetic pathways of hm^5Cm34 and f^5Cm34 in ct-$tRNA^{Leu}$(CAA). Initially, NSUN2 methylates C34 to form m^5C34 in the presence of AdoMet. ALKBH1 hydroxylates m^5C34 to form hm^5C34, and then oxidizes hm^5C34 to yield f^5C34. These reactions require O_2 and 2-OG as substrates. Precursor ct-$tRNA^{Leu}$(CAA) bearing hm^5C34 or f^5C34 is exported to the cytoplasm and methylated by FTSJ1 together with a partner protein (probably WDR6) in an AdoMet-dependent manner to form hm^5Cm34 or f^5Cm34, respectively. In *ALKBH1* KO cells (shaded), ct-$tRNA^{Leu}$(CAA) containing m^5C34 is exported to the cytoplasm, where it is methylated by FTSJ1 to form m^5Cm34.

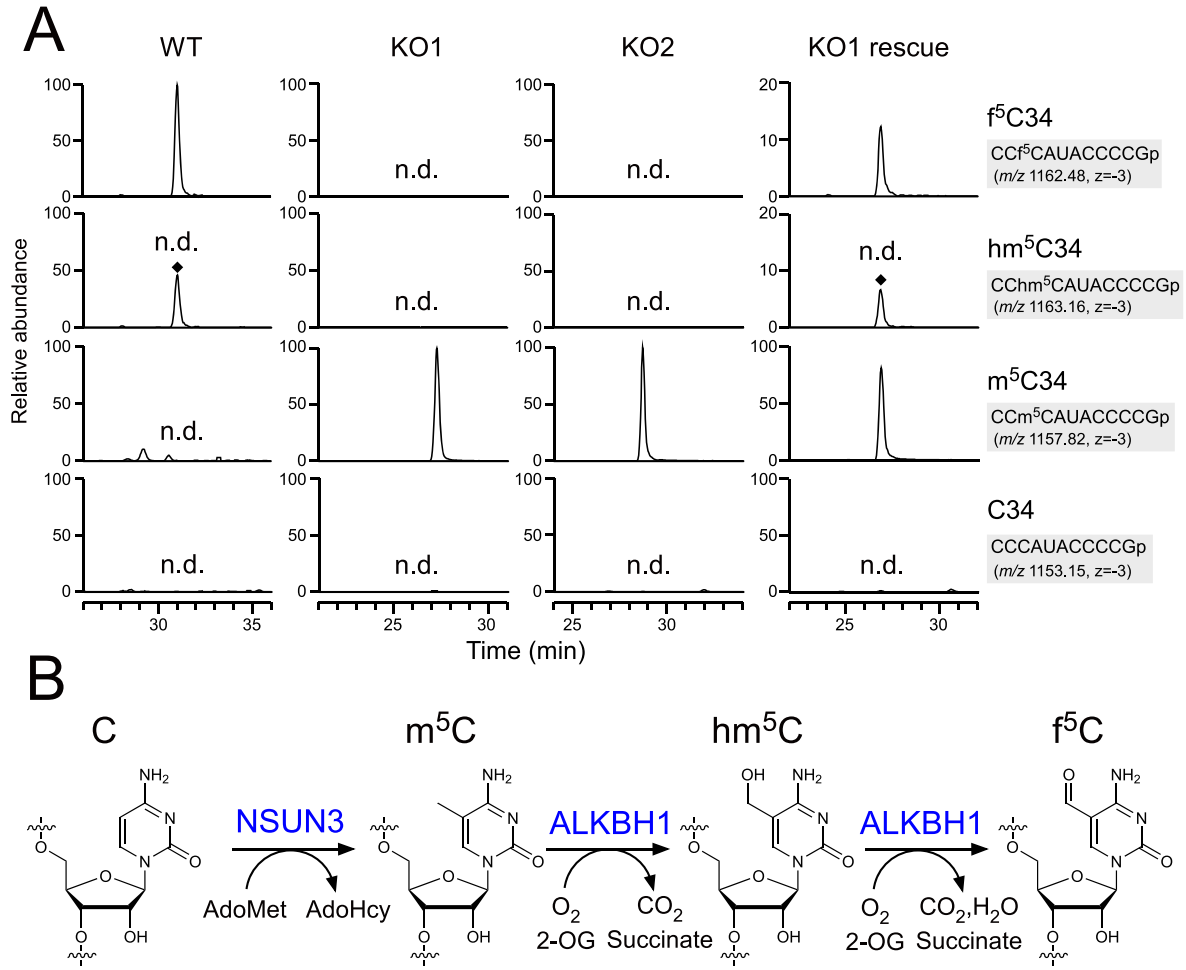

Figure 4. *ALKBH1* is essential for f^5C34 biogenesis in mt-$tRNA^{Met}$. (**A**) Mass chromatograms of the anticodon-containing fragments of mt-$tRNA^{Met}$ containing f^5C34 (top), hm^5C34 (second), m^5C34 (third) and C34 (bottom) isolated from WT, *ALKBH1* KO cell lines and KO1 rescued with plasmid-encoded *ALKBH1*. n.d., not detected. Filled diamonds in the second panels indicate a trace isotopic ion of the f^5C-containing fragment. (**B**) Biosynthetic pathway of f^5C34 in mt-$tRNA^{Met}$. NSUN3 methylates C34 to form m^5C34 in the presence of AdoMet. ALKBH1 hydroxylates m^5C34 to form hm^5C34, and then oxidizes hm^5C34 to yield f^5C34. These reactions require O_2 and 2-OG as substrates.

Impact of pathogenic point mutations on f^5C formation

According to MITOMAP, eight point mutations in the mt-$tRNA^{Met}$ gene are associated with human diseases (39). We previously reported two pathogenic mutations, A4435G and C4437U, that impaired m^5C34 formation by NSUN3, possibly causing hypomodification of f^5C34 (6). To determine whether these point mutations affect f^5C34 formation mediated by ALKBH1, mutant mt-$tRNAs^{Met}$ containing each of eight pathogenic mutations were prepared and methylated by NSUN3 to introduce as much m^5C34 as possible. Then, we examined *in vitro* hydroxylation and oxidation of m^5C34 in these mutant tRNAs by ALKBH1, but observed no obvious reduction of hm^5C34/f^5C34 formation (Figure 6D). This result suggests that none of the pathogenic point mutations in mt-$tRNA^{Met}$ tested here impair hydroxylation or oxidation of m^5C34 mediated by ALKBH1.

ALKBH1 is involved in demethylation of m^1A in mt-tRNAs

ALKBH1 can demethylate m^1A in ct-tRNAs (17). Given that ALKBH1 is localized in mitochondria (37), we asked whether mitochondrial ALKBH1 is also involved in demethylation of m^1A in mitochondrial RNAs. m^1A is present at positions 9, 16 and 58 of several tRNAs (7,40,41) and at position 947 of 16S rRNA (28). We isolated mt-tRNAs for Arg, Lys and Leu(UUR) from WT and *ALKBH1* KO cells, and compared the m^1A frequencies among them by measuring m^1A-containing fragments by RNA-MS (Figure 7AB and Supplementary Figure S2A–C). The frequency of m^1A16 in mt-$tRNA^{Arg}$ was higher in *ALKBH1* KO cells (33.3%), than in WT cells (17.9%) (Figure 7A). The level of m^1A58 in mt-$tRNA^{Lys}$ was also elevated in *ALKBH1* KO cells (Figure 7B). The increase in m^1A frequency at these sites in *ALKBH1* KO cells was also confirmed by primer extension (Figure 7CD). Other m^1A sites at positions 9 and 58 of mt-tRNAs were unchanged upon KO of *ALKBH1* (Supplementary Figure S2A–C). In particular, m^1A58 was fully

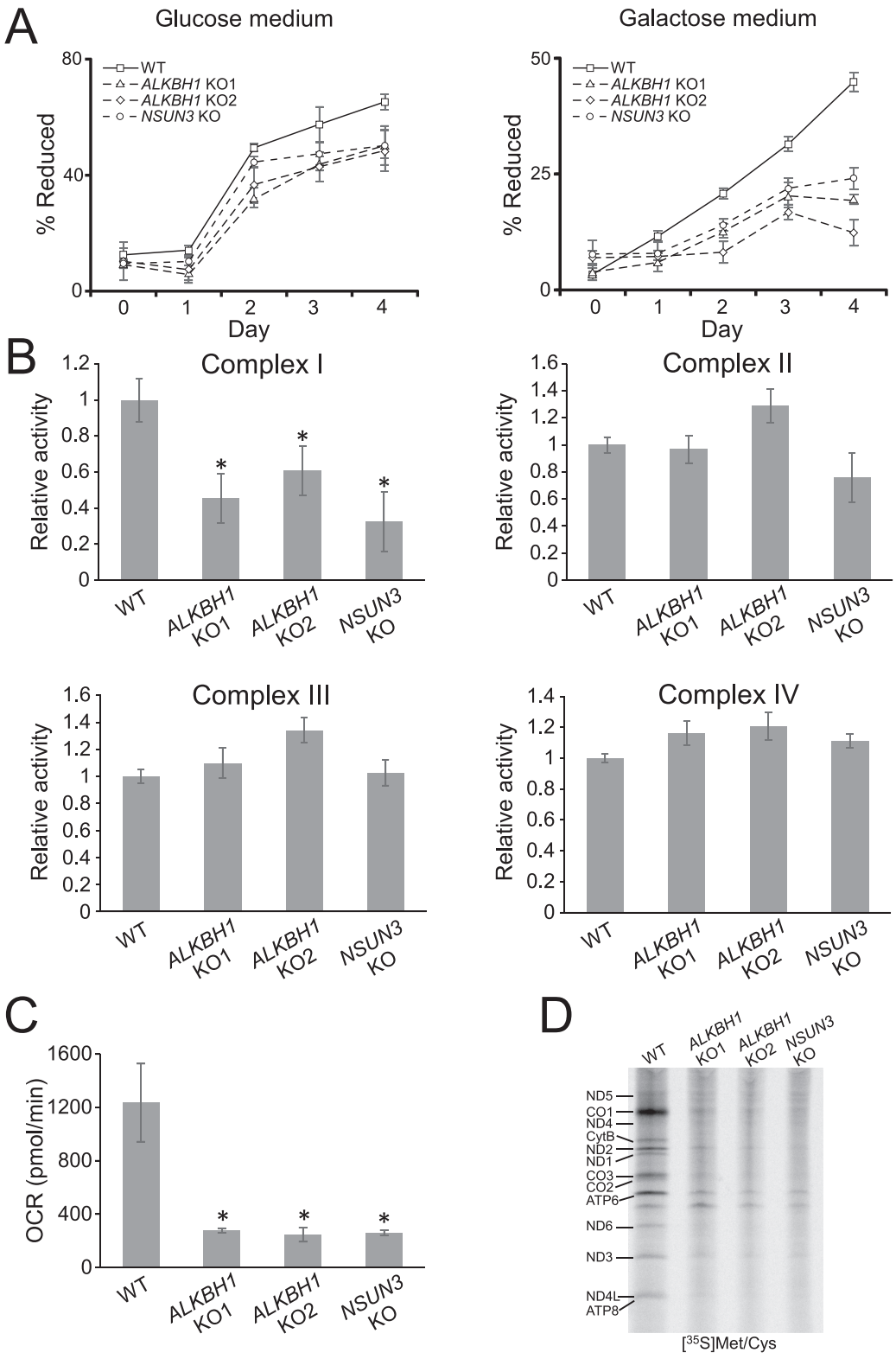

Figure 5. ALKBH1 is required for mitochondrial function. (**A**) Growth curves of WT, *ALKBH1* KO and *NSUN3* KO cells in a medium containing glucose (left panel) or galactose (right panel) as a primary carbon source. Mean values of five independent cultures are plotted; error bars indicate s.d. (**B**) Relative activities of respiratory chain complexes in WT, *ALKBH1* KO and *NSUN3* KO cells. Activity of each complex is normalized against the corresponding citrate synthase (CS) activity. Data are presented as mean ± SD. of three independent assays. $*P < 0.05$, Student's *t*-test. (**C**) Oxygen consumption rate of WT, *ALKBH1* KO and *NSUN3* KO cells, measured by an XF24 extracellular flux analyzer. Data are presented as mean ± SD. of three independent assays. $*P < 0.005$, Student's *t*-test. (**D**) Pulse labeling of mitochondrial protein synthesis in WT, *ALKBH1* KO and *NSUN3* KO cells. Under inhibition of cytoplasmic translation, mitochondrial protein synthesis was labeled with [^{35}S] Met and [^{35}S] Cys.

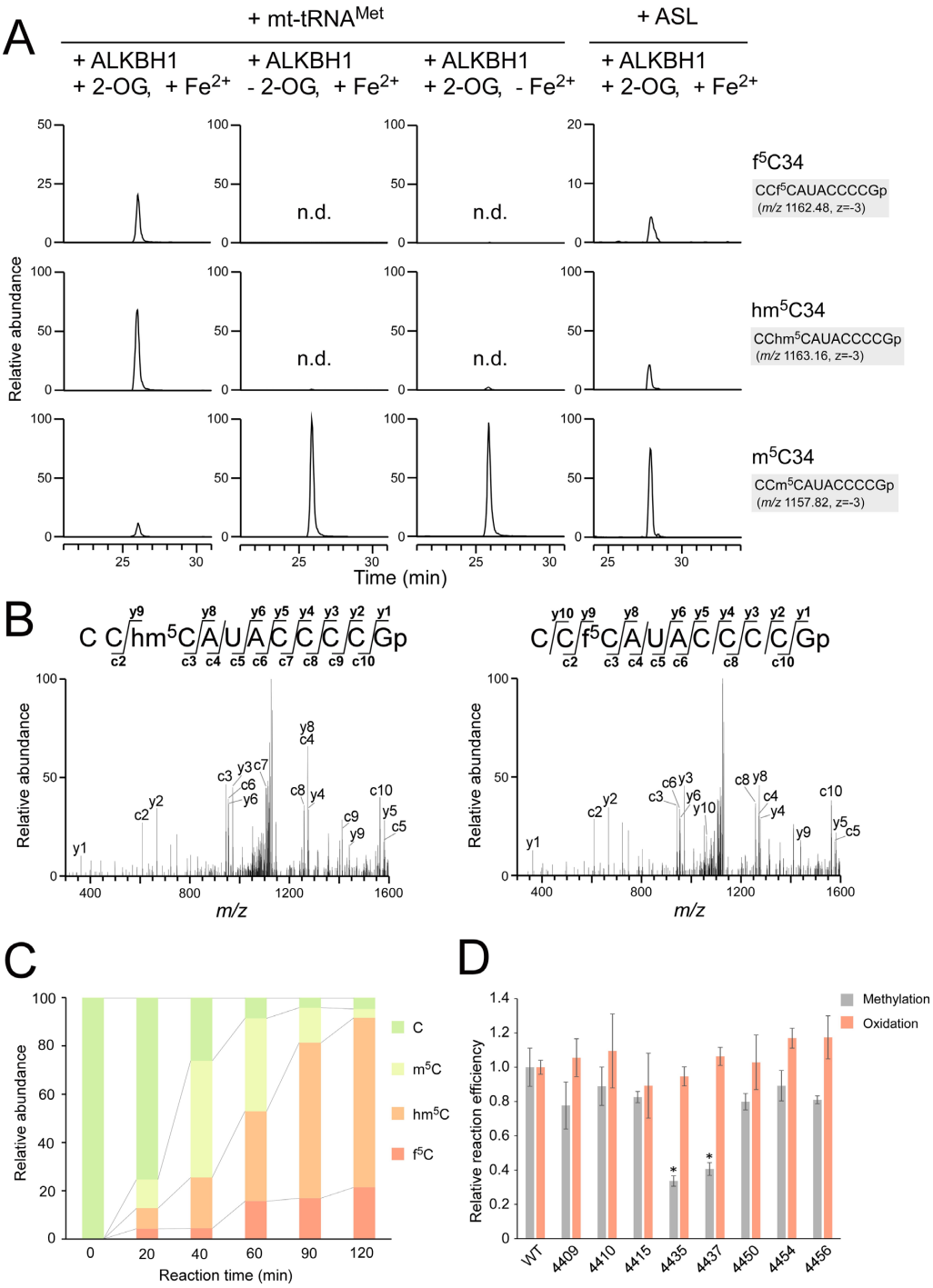

Figure 6. *In vitro* reconstitution of f^5C34 formation (**A**) Mass chromatograms of the anticodon-containing fragments of mt-$tRNA^{Met}$ and ASL to detect f^5C34 (top), hm^5C34 (middle) and m^5C34 (bottom) after *in vitro* reconstitution of f^5C34 with ALKBH1 in the presence or absence of 2-OG and Fe^{2+}. (**B**) CID spectra of the hm^5C34 (left)- and f^5C34 (right)-containing fragments reconstituted *in vitro*. The precursor ions are m/z 1163.48 and 1163.15 for hm^5C34 and f^5C34, respectively. Product ions are assigned on the corresponding sequences. (**C**) *In vitro* f^5C34 formation from C34 via consecutive reactions mediated by NSUN3 and ALKBH1. Time-dependent alteration of modification status in mt-$tRNA^{Met}$. Fractions of the RNase T_1-digested fragments bearing C34 (green), m^5C34 (pale green), hm^5C34 (pale orange) and f^5C34 (orange) at each time point were calculated based on peak heights of mass chromatograms. Because hm^5C has a molecular mass 2Da larger than that of f^5C, the frequency of hm^5C was calculated by subtracting the theoretical value of the second isotopic peak (+2) of the f^5C-containing fragment. (**D**) Methylation (gray bars) and oxidation (orange bars) efficiencies of mutant mt-$tRNAs^{Met}$ normalized against those of mt-$tRNA^{Met}$. Positions of pathogenic mutations in mt-$tRNA^{Met}$ are shown in Figure 1B. Methylation data were obtained from our previous study (6). Each mt-$tRNA^{Met}$ mutant containing m^5C34 was incubated with ALKBH1 in the presence of 2-OG and Fe^{2+}, followed by RNase T_1 digestion and subjected to RNA-MS. Reaction efficiency was calculated by summing the peak heights of the anticodon-containing fragments bearing hm^5C34 and f^5C34, normalized against the total peak heights of the three fragments (m^5C34, hm^5C34 and f^5C34). Frequency of hm^5C was calculated by subtracting the theoretical value of the second isotopic peak (+2) of the f^5C-containing fragment. Data are presented as means ± SD of three independent reactions. *$P < 0.001$, Student's t-test.

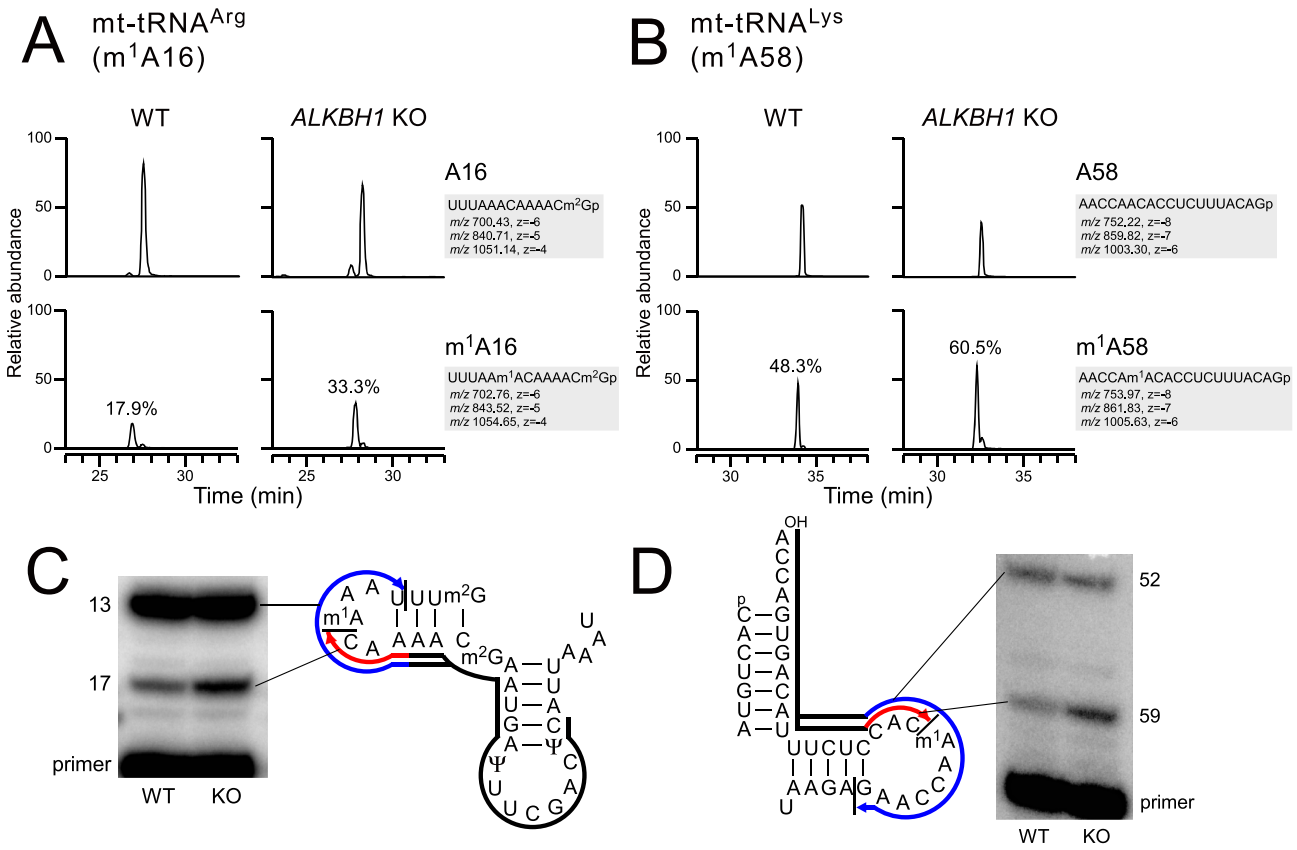

Figure 7. Level of m^1A in mt-tRNAs increased in *ALKBH1* KO cells (**A**) Mass chromatograms detecting negative ions ($z = -4$ to -6) of RNase T_1–digested fragments containing A16 (upper) and m^1A16 (lower) of mt-tRNA^{Arg} isolated from WT and *ALKBH1* KO cells. (**B**) Mass chromatograms detecting negative ions ($z = -6$ to -8) of RNase T_1–digested fragments containing A58 (upper) and m^1A58 (lower) of mt-tRNA^{Lys} isolated from WT and *ALKBH1* KO cells. (**C**) Detection of m^1A16 in mt-tRNA^{Arg} from WT and *ALKBH1* KO cells by primer extension. The primer is shown as a black line, and the extended cDNAs for detection of m^1A16 and A16 are depicted as red and blue lines, respectively. (**D**) Detection of m^1A58 in mt-tRNA^{Lys} from WT and *ALKBH1* KO cells by primer extension. The primer is shown as a black line, and the extended cDNAs for detection of m^1A58 and A58 are depicted as red and blue lines, respectively.

introduced in mt-tRNA^{Leu}(UAA), ct-tRNA^{Leu}(CAA), ct-tRNA^{Val}(AAC) and ct-tRNA^{Asn}(GUU) even in WT cells (Supplementary Figure S2C–F). Thus, ALKBH1 is not involved in demethylation of m^1A58 in these tRNAs. We also compared m^1A frequency at position 947 in 16S rRNA by primer extension analysis and found no significant change in the m^1A947 level between WT and *ALKBH1* KO cells (Supplementary Figure S2G).

DISCUSSION

Bacterial AlkB is a 2-OG- and Fe^{2+}-dependent dioxygenase that repairs alkylation damage, including m^1A and m^3C in DNA and RNA (42,43). In mammals, nine members of AlkB-family proteins (ALKBH1-8 and fat mass and obesity-associated protein (FTO)) have been identified (44–47), of which four are associated with RNA metabolism. FTO is the first RNA dioxygenase shown to have an 'eraser' function involved in demethylation of m^6A in mRNA in the cell (48), raising the possibility that m^6A is reversible. Recent work showed that FTO has a strong demethylation activity for m^6Am at the 5′ termini of capped mRNAs (49). ALKBH5 is another eraser for m^6A in mRNA (50). ALKBH8, a unique protein containing an AlkB domain fused to a tRNA methyltransferase domain, is involved in biogenesis of 5-methoxycarbonylhydroxymethyluridine ($mchm^5U34$) at the wobble position of ct-tRNAs (51,52). ALKBH3 has demethylation activity toward internal m^1A in mRNA (53,54), and recent work showed that ALKBH3 can demethylate m^6A in tRNAs (55), though exact position of m^6A in tRNA has not been determined yet.

ALKBH1, the first mammalian homolog of *E. coli* AlkB to be identified (44), is widely conserved among vertebrates and arthropods. ALKBH1 has demethylation activity toward m^3C in single-stranded DNA and RNA *in vitro* (37). ALKBH1 was once proposed to regulate neurodevelopment by demethylating histone H2A (33); however, this demethylation activity was not confirmed (16). Instead, it was proposed that ALKBH1 has the ability to demethylate m^6dA in DNA (16). A study published last year showed that ALKBH1 has a role in demethylating m^1A58 in ct-tRNAs (17), thus regulating protein synthesis by downregulating translation initiation and decreasing participation of tRNAs in the elongation stage. The physiological role of *ALKBH1* has been inferred based on phenotypic features of *Alkbh1*-null mice. A mouse harboring a deletion of exon 3 exhibited intra-uterine growth retardation with defective

placenta (56). By contrast, the exon 6 deletion mouse exhibited non-Mendelian inheritance of the targeted *Alkbh1* allele and sex-ratio distortion of the offspring (57), indicating that *ALKBH1* plays critical roles in the early development. Our finding of ALKBH1 as an RNA dioxygenase responsible for f^5C formation in cytoplasmic and mitochondrial tRNAs might provide insight into the enzyme's physiological role in mammals.

In this study, we showed that human ALKBH1 catalyzes hydroxylation and oxidization of m^5C34 in both ct-$tRNA^{Leu}$(CAA) and mt-$tRNA^{Met}$. These findings demonstrated that nuclear ALKBH1 and mitochondrial ALKBH1 play distinct roles in tRNA modifications. Although we elucidated the biogenesis of f^5Cm34 and hm^5Cm34 in ct-$tRNA^{Leu}$(CAA), the functions of these modifications remain obscure. Based on the functional importance of f^5C34 in mt-$tRNA^{Met}$, f^5Cm34/hm^5Cm34 might contribute to decoding of UUA as well as UUG. These modifications are thought to contribute to robust decoding of UUA, together with an isoacceptor $tRNA^{Leu}$ bearing a modified uridine at the wobble position (U*34), which is responsible for decoding UUR. In our RNA-MS analyses (Figures 2B and 3D), we measured the exact frequency of the wobble modifications in ct-$tRNAs^{Leu}$(CAA) isolated from mouse fetus and HEK293T cells (Supplementary Table S2), and observed that modification status differed between these two tRNAs. Mouse fetus ct-$tRNAs^{Leu}$(CAA) (mature form) contained 14% f^5Cm34 and 79% hm^5Cm, whereas human ct-$tRNAs^{Leu}$(CAA) isolated from HEK293T had 30% f^5Cm34, 26% hm^5Cm34 and 34% hm^5C34. These results suggest that the ratio of f^5Cm34 and hm^5Cm34 can be altered in various tissues and cells, indicating that their modification status is dynamically regulated in various physiological contexts. If f^5Cm34 and hm^5Cm34 play distinct roles in decoding, cytoplasmic protein synthesis could be regulated by the alterative wobble modifications. In addition, we found that f^5C34 is 2′-*O*-methylated more robustly than hm^5C34 (Supplementary Table S2). Considering that FTSJ1 is predominantly localized in the cytoplasm (34) (The Human Protein Atlas, http://www.proteinatlas.org/), precursor $tRNA^{Leu}$(CAA) bearing f^5C34 might be exported to the cytoplasm more efficiently than the tRNA bearing hm^5C34. Otherwise, FTSJ1 and its partner protein (probably WDR6), which determines specificity to position 34, might prefer f^5C34 over hm^5C34 for 2′-*O*-methylation. Pathogenic mutations in *FTSJ1* and *NSUN2* are associated with intellectual disabilities (58–62). Thus, dysregulation of protein synthesis caused by loss of f^5Cm34/hm^5Cm34 in ct-$tRNA^{Leu}$(CAA) might contribute to molecular pathogenesis of these diseases.

In the case of ct-$tRNA^{Leu}$(CAA), NSUN2 introduces m^5C34 to initiate formation of f^5Cm34/hm^5Cm34. By contrast, NSUN3 forms m^5C34 to initiate f^5C34 formation in mt-$tRNA^{Met}$. However, we found that hydroxylation and oxidation of m^5C34 in both tRNAs are commonly catalyzed by ALKBH1. *ALKBH1* KO cells exhibited slow growth in galactose medium, reduced Complex I activity and low oxygen consumption, indicating that the physiological role of ALKBH1 is connected with mitochondrial function. Because *ALKBH1* KO cells exhibited phenotypes similar to those of *NSUN3* KO cells, loss of f^5C34 is likely to be a primary cause of mitochondrial dysfunction of *ALKBH1* KO cells. Both *NSUN3* KO and *ALKBH1* KO cells exhibited Complex I deficiency, indicating that f^5C34 in mt-$tRNA^{Met}$ is required for efficient mitochondrial translation of protein components for Complex I. In fact, we also observed severe reduction of mitochondrial translation in *ALKBH1* KO cells. In support of this finding, steady state levels of ND2 and ND5 decreased, and assembly of Complex I was defective, in *NSUN3* KO cells (6). Because mt-$tRNA^{Met}$ contains m^5C34 in *ALKBH1* KO cells, m^5C34 appears to have no ability to decode AUA, as observed for C34 in *NSUN3* KO cells.

Previous studies reported that mt-$tRNA^{Met}$ contains m^5C34 in human culture cells. Haag *et al.* (15) performed bisulfite sequencing of total RNA from HeLa cells with or without $NaBH_4$ treatment, and found that a majority of the modification is f^5C34, whereas m^5C34 is actually present in mt-$tRNA^{Met}$ in HeLa cells. Van Haute *et al.* (13) used fCAB RNA-seq and RedBS RNA-seq to estimate that mt-$tRNA^{Met}$ isolated from human fibroblast contained 36–38% f^5C34 and ∼30% m^5C. Because both reports analyzed modification status by indirect methods, which may suffer from bias resulting in erroneous measurement of the frequency of each modification, we assume that the abundance of m^5C34 in mt-$tRNA^{Met}$ was overestimated in both cases. Otherwise, m^5C34 might have been detected in primary transcripts or precursors of mt-$tRNA^{Met}$. We isolated mt-$tRNA^{Met}$ from HEK293T and HeLa cells, and directly analyzed anticodon-containing fragments by LC/MS to determine the exact frequency of each modification. We could detect the RNA fragments containing C34, m^5C34, hm^5C34,or f^5C34 separately, based on their exact molecular masses. RNA fragments are ionized by ESI as negative ions derived from phosphate groups. Hence, ionization efficiencies of RNA fragments bearing the same sequences, but different modifications, do not significantly differ in general, because ESI ionization relies mainly on numbers of phosphate groups, rather than the type of base modifications (23). The relative amounts of these fragments can be calculated by their detection intensities. Using this method, we demonstrated that mt-$tRNA^{Met}$ is fully modified with f^5C34 in both HEK293T (Figure 4A) and HeLa cells (Supplementary Figure S3). No hypomodified fragment bearing C34, m^5C34 or hm^5C34 was detected in mature mt-$tRNA^{Met}$, which participates in translation. However, we cannot rule out the possibility that f^5C34 is dynamically regulated in different tissues and cells via alternative expression of *NSUN3* and *ALKBH1*, or due to an intracellular change in concentrations of AdoMet, Fe^{2+}, 2-OG and O_2.

In vitro reconstitution of f^5C34 revealed that ALKBH1 catalyzes hydroxylation and oxidation of m^5C34 in the presence of 2-OG and Fe^{2+} (Figure 6A). In addition, we successfully reconstituted f^5C34 from C34 by consecutive reactions catalyzed by NSUN3 and ALKBH1. Over the course of these reactions, m^5C34 was formed rapidly, followed by the appearance of hm^5C34 and ultimately f^5C34 gradually accumulated, but no 5-carboxycytidine (ca^5C34) was formed. This reaction profile indicates that ALKBH1 catalyzes two-step reactions initiated by hydroxylation of m^5C34 to form

hm^{5}C34, and followed by oxidation of hm^{5}C34 to form f^{5}C34. Haag *et al.* (15) only detected f^{5}C34 as an oxidation product of m^{5}C34 in ASL *in vitro* and did not detect any hm^{5}C34 as an intermediate. This discrepancy might arise due to differences in our assay conditions or recombinant protein constructs. In genomic DNA, the TET family enzymes, another family of Fe^{2+}/2-OG-dependent oxygenases, hydroxylate m^{5}dC to form hm^{5}dC as a major product (63,64). TET enzymes can also oxidize m^{5}C in RNA to form hm^{5}C *in vitro* as well as in human culture cells (65). In *Drosophila*, hm^{5}C in RNA is synthesized by dTet (66), indicating that TET enzymes also participate in the formation of hm^{5}C in RNA. However, hm^{5}Cm in ct-tRNA^{Leu}(CAA) was completely absent in the *ALKBH1* KO cells used in this study, ruling out a possibility that TET enzymes are redundantly involved in this process. Considering that the target sites of ALKBH1 reside in loop regions of RNA hairpins (17), ALKBH1 might oxidize m^{5}C to form hm^{5}C or f^{5}C in the loop regions of mRNAs.

We also investigated whether ALKBH1 is involved in demethylation of m^{1}A in mitochondria and found that the m^{1}A frequency at two sites (m^{1}A16 in mt-tRNA^{Arg} and m^{1}A58 in mt-tRNA^{Lys}) was elevated (Figure 7), whereas four other sites in mt RNAs were unchanged, upon *ALKBH1* KO (Supplementary Figure S2A–C and G). m^{1}A16 and m^{1}A58 are found in the loop regions of the D-stem and T-stem, respectively. No m^{1}A at position 9 was targeted by ALKBH1. Taken together with the formation of f^{5}C34, these results indicate that ALKBH1 prefers to recognize the stem-loop structure of RNA and oxidize the target methyl group. We previously reported that m^{1}A58 in mt-tRNAs is introduced by Trmt61B (27). However, knockdown of this gene in HeLa cells caused no obvious phenotype. Thus, regulation of m^{1}A58 by ALKBH1 might have a moderate effect in mitochondrial function, and the mitochondrial dysfunction observed in *ALKBH1* KO cells should be largely attributed to the loss of f^{5}C34 in mt-tRNA^{Met}.

In this study, we found that ALKBH1 is responsible for biogenesis of hm^{5}Cm34/f^{5}Cm34 in ct-tRNA^{Leu}(CAA), as well as f^{5}C34 in mt-tRNA^{Met}. *ALKBH1* KO cells exhibited strong reduction in mitochondrial translation and reduced respiratory complex activities, demonstrating that ALKBH1-mediated f^{5}C34 formation is required for mitochondrial functions. *In vitro* reconstitution of f^{5}C34 revealed that ALKBH1 first hydroxylates m^{5}C34 to form hm^{5}C34, and then oxidizes hm^{5}C34 to form f^{5}C34. We also found two m^{1}A sites in mt-tRNAs that were present at higher frequencies in *ALKBH1* KO cells, indicating that mitochondrial ALKBH1 is also involved in m^{1}A demethylation.

SUPPLEMENTARY DATA

Supplementary Data are available at NAR Online.

ACKNOWLEDGEMENTS

We are grateful to all members of the Suzuki laboratory, especially to Y. Yashiro, K. Asano, R. Okita and Y. Sakaguchi, for their technical assistance and fruitful discussion. We thank S. Nakano, N. Mizushima (University of Tokyo), K. Tomizawa and F. Wei (Kumamoto University) for their kind support for measuring mitochondrial activities, and I. Hatada and T. Horii (Gunma University) for kindly providing materials. Special thanks are due to Chuan He and Tao Pan (University of Chicago) for informing us of their unpublished results.

FUNDING

Grants-in-Aid for Scientific Research on Priority Areas from the Ministry of Education, Culture, Sports, Science, and Technology of Japan (MEXT); Japan Society for the Promotion of Science (JSPS) [26113003 and 26220205 to Ts.S., 26702035 to Ta.S.]. Funding for open access charge: JSPS; Grants-in-Aid for Scientific Research on Priority Areas from the Ministry of Education, Culture, Sports, Science, and Technology of Japan.
Conflict of interest statement. None declared.

REFERENCES

1. Machnicka,M.A., Milanowska,K., Osman Oglou,O., Purta,E., Kurkowska,M., Olchowik,A., Januszewski,W., Kalinowski,S., Dunin-Horkawicz,S., Rother,K.M. *et al.* (2013) MODOMICS: a database of RNA modification pathways–2013 update. *Nucleic Acids Res.*, **41**, D262–D267.
2. Bjork,G. (1995) Biosynthesis and function of modified nucleosides. In: Soll,D and RajBhandary,UL (eds). *tRNA: Structure, Biosynthesis, and Function*. American Society for Microbiology, Washington, D.C., pp. 165–205.
3. Suzuki,T. (2005) Biosynthesis and Function of tRNA Wobble Modifications. In: Grosjean,H (ed). *Fine-Tuning of RNA Functions by Modification and Editing*. Springer-Verlag Berlin and Heidelberg GmbH & Co. KG, Berlin Heidelberg, Vol. **12**, pp. 23–69.
4. Moriya,J., Yokogawa,T., Wakita,K., Ueda,T., Nishikawa,K., Crain,P.F., Hashizume,T., Pomerantz,S.C., McCloskey,J.A., Kawai,G. *et al.* (1994) A novel modified nucleoside found at the first position of the anticodon of methionine tRNA from bovine liver mitochondria. *Biochemistry*, **33**, 2234–2239.
5. Watanabe,Y., Tsurui,H., Ueda,T., Furushima,R., Takamiya,S., Kita,K., Nishikawa,K. and Watanabe,K. (1994) Primary and higher order structures of nematode (Ascaris suum) mitochondrial tRNAs lacking either the T or D stem. *J. Biol. Chem.*, **269**, 22902–22906.
6. Nakano,S., Suzuki,T., Kawarada,L., Iwata,H. and Asano,K. (2016) NSUN3 methylase initiates 5-formylcytidine biogenesis in human mitochondrial tRNA(Met). *Nat. Chem. Biol.*, **12**, 546–551.
7. Suzuki,T., Nagao,A. and Suzuki,T. (2011) Human mitochondrial tRNAs: biogenesis, function, structural aspects, and diseases. *Annu. Rev. Genet.*, **45**, 299–329.
8. Takemoto,C., Spremulli,L.L., Benkowski,L.A., Ueda,T., Yokogawa,T. and Watanabe,K. (2009) Unconventional decoding of the AUA codon as methionine by mitochondrial tRNA^{Met} with the anticodon f^{5}CAU as revealed with a mitochondrial in vitro translation system. *Nucleic Acids Res.*, **37**, 1616–1627.
9. Cantara,W.A., Murphy,F.V.t., Demirci,H. and Agris,P.F. (2013) Expanded use of sense codons is regulated by modified cytidines in tRNA. *Proc. Natl. Acad. Sci. U.S.A.*, **110**, 10964–10969.
10. Lu,Z., Chen,H., Meng,Y., Wang,Y., Xue,L., Zhi,S., Qiu,Q., Yang,L., Mo,J.Q. and Guan,M.X. (2011) The tRNAMet 4435A>G mutation in the mitochondrial haplogroup G2a1 is responsible for maternally inherited hypertension in a Chinese pedigree. *Eur. J. Hum. Genet.*, **19**, 1181–1186.
11. Qu,J., Li,R., Zhou,X., Tong,Y., Lu,F., Qian,Y., Hu,Y., Mo,J.Q., West,C.E. and Guan,M.X. (2006) The novel A4435G mutation in the mitochondrial tRNA^{Met} may modulate the phenotypic expression of the LHON-associated ND4 G11778A mutation. *Invest. Ophthalmol. Vis. Sci.*, **47**, 475–483.
12. Tang,S., Wang,J., Zhang,V.W., Li,F.Y., Landsverk,M., Cui,H., Truong,C.K., Wang,G., Chen,L.C., Graham,B. *et al.* (2013)

Transition to next generation analysis of the whole mitochondrial genome: a summary of molecular defects. *Hum. Mutat.*, **34**, 882–893.
13. Van Haute,L., Dietmann,S., Kremer,L., Hussain,S., Pearce,S.F., Powell,C.A., Rorbach,J., Lantaff,R., Blanco,S., Sauer,S. *et al.* (2016) Deficient methylation and formylation of mt-tRNA(Met) wobble cytosine in a patient carrying mutations in NSUN3. *Nat. Commun.*, **7**, 12039.
14. Van Haute,L., Powell,C.A. and Minczuk,M. (2017) Dealing with an unconventional genetic code in mitochondria: the biogenesis and pathogenic defects of the 5-formylcytosine modification in mitochondrial $tRNA^{Met}$. *Biomolecules*, **7**, doi:10.3390/biom7010024.
15. Haag,S., Sloan,K.E., Ranjan,N., Warda,A.S., Kretschmer,J., Blessing,C., Hubner,B., Seikowski,J., Dennerlein,S., Rehling,P. *et al.* (2016) NSUN3 and ABH1 modify the wobble position of mt-$tRNA^{Met}$ to expand codon recognition in mitochondrial translation. *EMBO J.*, **35**, 2104–2119.
16. Wu,T.P., Wang,T., Seetin,M.G., Lai,Y., Zhu,S., Lin,K., Liu,Y., Byrum,S.D., Mackintosh,S.G., Zhong,M. *et al.* (2016) DNA methylation on N (6)-adenine in mammalian embryonic stem cells. *Nature*, **532**, 329–333.
17. Liu,F., Clark,W., Luo,G., Wang,X., Fu,Y., Wei,J., Hao,Z., Dai,Q., Zheng,G., Ma,H. *et al.* (2016) ALKBH1-mediated tRNA demethylation regulates translation. *Cell*, **167**, 816–828.
18. Pais de Barros,J.P., Keith,G., El Adlouni,C., Glasser,A.L., Mack,G., Dirheimer,G. and Desgres,J. (1996) 2′-*O*-methyl-5-formylcytidine (f^5Cm), a new modified nucleotide at the 'wobble' of two cytoplasmic $tRNAs^{Leu\ (NAA)}$ from bovine liver. *Nucleic Acids Res.*, **24**, 1489–1496.
19. Huber,S.M., van Delft,P., Mendil,L., Bachman,M., Smollett,K., Werner,F., Miska,E.A. and Balasubramanian,S. (2015) Formation and abundance of 5-hydroxymethylcytosine in RNA. *Chembiochem*, **16**, 752–755.
20. Ran,F.A., Hsu,P.D., Wright,J., Agarwala,V., Scott,D.A. and Zhang,F. (2013) Genome engineering using the CRISPR-Cas9 system. *Nat. Protoc.*, **8**, 2281–2308.
21. Miyauchi,K., Ohara,T. and Suzuki,T. (2007) Automated parallel isolation of multiple species of non-coding RNAs by the reciprocal circulating chromatography method. *Nucleic Acids Res.*, **35**, e24.
22. Miyauchi,K., Kimura,S. and Suzuki,T. (2013) A cyclic form of N^6-threonylcarbamoyladenosine as a widely distributed tRNA hypermodification. *Nat. Chem. Biol.*, **9**, 105–111.
23. Ohira,T. and Suzuki,T. (2016) Precursors of tRNAs are stabilized by methylguanosine cap structures. *Nat. Chem. Biol.*, **12**, 648–655.
24. Suzuki,T., Ikeuchi,Y., Noma,A., Suzuki,T. and Sakaguchi,Y. (2007) Mass spectrometric identification and characterization of RNA-modifying enzymes. *Meth. Enzymol.*, **425**, 211–229.
25. Milligan,J.F., Groebe,D.R., Witherell,G.W. and Uhlenbeck,O.C. (1987) Oligoribonucleotide synthesis using T7 RNA polymerase and synthetic DNA templates. *Nucleic Acids Res.*, **15**, 8783–8798.
26. Trounce,I.A., Kim,Y.L., Jun,A.S. and Wallace,D.C. (1996) Assessment of mitochondrial oxidative phosphorylation in patient muscle biopsies, lymphoblasts, and transmitochondrial cell lines. *Meth. Enzymol.*, **264**, 484–509.
27. Chujo,T. and Suzuki,T. (2012) Trmt61B is a methyltransferase responsible for 1-methyladenosine at position 58 of human mitochondrial tRNAs. *RNA*, **18**, 2269–2276.
28. Bar-Yaacov,D., Frumkin,I., Yashiro,Y., Chujo,T., Ishigami,Y., Chemla,Y., Blumberg,A., Schlesinger,O., Bieri,P., Greber,B. *et al.* (2016) Mitochondrial 16S rRNA is methylated by tRNA methyltransferase TRMT61B in all vertebrates. *PLoS Biol.*, **14**, e1002557.
29. Strobel,M.C. and Abelson,J. (1986) Effect of intron mutations on processing and function of Saccharomyces cerevisiae SUP53 tRNA *in vitro and in vivo. Mol. Cell. Biol.*, **6**, 2663–2673.
30. Karwowska,U. and Szweykowska-Kulinska,Z. (1997) New intron-containing human tRNA(Leu) genes. *Acta Biochim. Pol.*, **44**, 791–794.
31. Motorin,Y. and Grosjean,H. (1999) Multisite-specific tRNA:m^5C-methyltransferase (Trm4) in yeast Saccharomyces cerevisiae: identification of the gene and substrate specificity of the enzyme. *RNA*, **5**, 1105–1118.
32. Brzezicha,B., Schmidt,M., Makalowska,I., Jarmolowski,A., Pienkowska,J. and Szweykowska-Kulinska,Z. (2006) Identification of human tRNA:m^5C methyltransferase catalysing intron-dependent m^5C formation in the first position of the anticodon of the pre-$tRNA^{Leu}_{(CAA)}$. *Nucleic Acids Res.*, **34**, 6034–6043.
33. Ougland,R., Lando,D., Jonson,I., Dahl,J.A., Moen,M.N., Nordstrand,L.M., Rognes,T., Lee,J.T., Klungland,A., Kouzarides,T. *et al.* (2012) ALKBH1 is a histone H2A dioxygenase involved in neural differentiation. *Stem Cells*, **30**, 2672–2682.
34. Pintard,L., Lecointe,F., Bujnicki,J.M., Bonnerot,C., Grosjean,H. and Lapeyre,B. (2002) Trm7p catalyses the formation of two 2′-*O*-methylriboses in yeast tRNA anticodon loop. *EMBO J.*, **21**, 1811–1820.
35. Guy,M.P., Shaw,M., Weiner,C.L., Hobson,L., Stark,Z., Rose,K., Kalscheuer,V.M., Gecz,J. and Phizicky,E.M. (2015) Defects in tRNA anticodon loop 2′-*O*-methylation are implicated in nonsyndromic X-linked intellectual disability due to mutations in FTSJ1. *Hum. Mutat.*, **36**, 1176–1187.
36. Guy,M.P., Podyma,B.M., Preston,M.A., Shaheen,H.H., Krivos,K.L., Limbach,P.A., Hopper,A.K. and Phizicky,E.M. (2012) Yeast Trm7 interacts with distinct proteins for critical modifications of the tRNAPhe anticodon loop. *RNA*, **18**, 1921–1933.
37. Westbye,M.P., Feyzi,E., Aas,P.A., Vagbo,C.B., Talstad,V.A., Kavli,B., Hagen,L., Sundheim,O., Akbari,M., Liabakk,N.B. *et al.* (2008) Human AlkB homolog 1 is a mitochondrial protein that demethylates 3-methylcytosine in DNA and RNA. *J. Biol. Chem.*, **283**, 25046–25056.
38. Robinson,B.H., Petrova-Benedict,R., Buncic,J.R. and Wallace,D.C. (1992) Nonviability of cells with oxidative defects in galactose medium: a screening test for affected patient fibroblasts. *Biochem. Med. Metab. Biol.*, **48**, 122–126.
39. Lott,M.T., Leipzig,J.N., Derbeneva,O., Xie,H.M., Chalkia,D., Sarmady,M., Procaccio,V. and Wallace,D.C. (2002) *Current Protocols in Bioinformatics*. John Wiley & Sons, Inc., New Jersey.
40. Clark,W.C., Evans,M.E., Dominissini,D., Zheng,G. and Pan,T. (2016) tRNA base methylation identification and quantification via high-throughput sequencing. *RNA*, **22**, 1771–1784.
41. Suzuki,T. (2014) A complete landscape of post-transcriptional modifications in mammalian mitochondrial tRNAs. *Nucleic Acids Res.*, **42**, 7346–7357.
42. Falnes,P.O., Johansen,R.F. and Seeberg,E. (2002) AlkB-mediated oxidative demethylation reverses DNA damage in *Escherichia coli*. *Nature*, **419**, 178–182.
43. Aas,P.A., Otterlei,M., Falnes,P.O., Vagbo,C.B., Skorpen,F., Akbari,M., Sundheim,O., Bjoras,M., Slupphaug,G., Seeberg,E. *et al.* (2003) Human and bacterial oxidative demethylases repair alkylation damage in both RNA and DNA. *Nature*, **421**, 859–863.
44. Wei,Y.F., Carter,K.C., Wang,R.P. and Shell,B.K. (1996) Molecular cloning and functional analysis of a human cDNA encoding an *Escherichia coli* AlkB homolog, a protein involved in DNA alkylation damage repair. *Nucleic Acids Res.*, **24**, 931–937.
45. Duncan,T., Trewick,S.C., Koivisto,P., Bates,P.A., Lindahl,T. and Sedgwick,B. (2002) Reversal of DNA alkylation damage by two human dioxygenases. *Proc. Natl. Acad. Sci. U.S.A.*, **99**, 16660–16665.
46. Kurowski,M.A., Bhagwat,A.S., Papaj,G. and Bujnicki,J.M. (2003) Phylogenomic identification of five new human homologs of the DNA repair enzyme AlkB. *BMC Genomics*, **4**, 48.
47. Gerken,T., Girard,C.A., Tung,Y.C., Webby,C.J., Saudek,V., Hewitson,K.S., Yeo,G.S., McDonough,M.A., Cunliffe,S., McNeill,L.A. *et al.* (2007) The obesity-associated FTO gene encodes a 2-oxoglutarate-dependent nucleic acid demethylase. *Science*, **318**, 1469–1472.
48. Jia,G., Fu,Y., Zhao,X., Dai,Q., Zheng,G., Yang,Y., Yi,C., Lindahl,T., Pan,T., Yang,Y.G. *et al.* (2011) N^6-methyladenosine in nuclear RNA is a major substrate of the obesity-associated FTO. *Nat. Chem. Biol.*, **7**, 885–887.
49. Mauer,J., Luo,X., Blanjoie,A., Jiao,X., Grozhik,A.V., Patil,D.P., Linder,B., Pickering,B.F., Vasseur,J.J., Chen,Q. *et al.* (2017) Reversible methylation of m^6Am in the 5′ cap controls mRNA stability. *Nature*, **541**, 371–375.
50. Zheng,G., Dahl,J.A., Niu,Y., Fedorcsak,P., Huang,C.M., Li,C.J., Vagbo,C.B., Shi,Y., Wang,W.L., Song,S.H. *et al.* (2013) ALKBH5 is a mammalian RNA demethylase that impacts RNA metabolism and mouse fertility. *Mol. Cell*, **49**, 18–29.
51. Fu,Y., Dai,Q., Zhang,W., Ren,J., Pan,T. and He,C. (2010) The AlkB domain of mammalian ABH8 catalyzes hydroxylation of

5-methoxycarbonylmethyluridine at the wobble position of tRNA. *Angew. Chem. Int. Ed. Engl.*, **49**, 8885–8888.
52. Songe-Moller,L., van den Born,E., Leihne,V., Vagbo,C.B., Kristoffersen,T., Krokan,H.E., Kirpekar,F., Falnes,P.O. and Klungland,A. (2010) Mammalian ALKBH8 possesses tRNA methyltransferase activity required for the biogenesis of multiple wobble uridine modifications implicated in translational decoding. *Mol. Cell. Biol.*, **30**, 1814–1827.
53. Li,X., Xiong,X., Wang,K., Wang,L., Shu,X., Ma,S. and Yi,C. (2016) Transcriptome-wide mapping reveals reversible and dynamic N (1)-methyladenosine methylome. *Nat. Chem. Biol.*, **12**, 311–316.
54. Dominissini,D., Nachtergaele,S., Moshitch-Moshkovitz,S., Peer,E., Kol,N., Ben-Haim,M.S., Dai,Q., Di Segni,A., Salmon-Divon,M., Clark,W.C. *et al.* (2016) The dynamic N (1)-methyladenosine methylome in eukaryotic messenger RNA. *Nature*, **530**, 441–446.
55. Ueda,Y., Ooshio,I., Fusamae,Y., Kitae,K., Kawaguchi,M., Jingushi,K., Hase,H., Harada,K., Hirata,K. and Tsujikawa,K. (2017) AlkB homolog 3-mediated tRNA demethylation promotes protein synthesis in cancer cells. *Sci. Rep.*, **7**, 42271.
56. Pan,Z., Sikandar,S., Witherspoon,M., Dizon,D., Nguyen,T., Benirschke,K., Wiley,C., Vrana,P. and Lipkin,S.M. (2008) Impaired placental trophoblast lineage differentiation in Alkbh1(-/-) mice. *Dev. Dyn.*, **237**, 316–327.
57. Nordstrand,L.M., Svard,J., Larsen,E., Nilsen,A., Ougland,R., Furu,K., Lien,G.F., Rognes,T., Namekawa,S.H., Lee,J.T. *et al.* (2010) Mice lacking *Alkbh1* display sex-ratio distortion and unilateral eye defects. *PLoS One*, **5**, e13827.
58. Freude,K., Hoffmann,K., Jensen,L.R., Delatycki,M.B., des Portes,V., Moser,B., Hamel,B., van Bokhoven,H., Moraine,C., Fryns,J.P. *et al.* (2004) Mutations in the FTSJ1 gene coding for a novel S-adenosylmethionine-binding protein cause nonsyndromic X-linked mental retardation. *Am. J. Hum. Genet.*, **75**, 305–309.
59. Takano,K., Nakagawa,E., Inoue,K., Kamada,F., Kure,S. and Goto,Y. (2008) A loss-of-function mutation in the FTSJ1 gene causes nonsyndromic X-linked mental retardation in a Japanese family. *Am. J. Med. Genet.*, **147**, 479–484.
60. Khan,M.A., Rafiq,M.A., Noor,A., Hussain,S., Flores,J.V., Rupp,V., Vincent,A.K., Malli,R., Ali,G., Khan,F.S. *et al.* (2012) Mutation in *NSUN2*, which encodes an RNA methyltransferase, causes autosomal-recessive intellectual disability. *Am. J. Hum. Genet.*, **90**, 856–863.
61. Martinez,F.J., Lee,J.H., Lee,J.E., Blanco,S., Nickerson,E., Gabriel,S., Frye,M., Al-Gazali,L. and Gleeson,J.G. (2012) Whole exome sequencing identifies a splicing mutation in *NSUN2* as a cause of a Dubowitz-like syndrome. *J. Med. Genet.*, **49**, 380–385.
62. Abbasi-Moheb,L., Mertel,S., Gonsior,M., Nouri-Vahid,L., Kahrizi,K., Cirak,S., Wieczorek,D., Motazacker,M.M., Esmaeeli-Nieh,S., Cremer,K. *et al.* (2012) Mutations in *NSUN2* cause autosomal-recessive intellectual disability. *Am. J. Hum. Genet.*, **90**, 847–855.
63. Tahiliani,M., Koh,K.P., Shen,Y., Pastor,W.A., Bandukwala,H., Brudno,Y., Agarwal,S., Iyer,L.M., Liu,D.R., Aravind,L. *et al.* (2009) Conversion of 5-methylcytosine to 5-hydroxymethylcytosine in mammalian DNA by MLL partner TET1. *Science*, **324**, 930–935.
64. Ito,S., Shen,L., Dai,Q., Wu,S.C., Collins,L.B., Swenberg,J.A., He,C. and Zhang,Y. (2011) Tet proteins can convert 5-methylcytosine to 5-formylcytosine and 5-carboxylcytosine. *Science*, **333**, 1300–1303.
65. Fu,L., Guerrero,C.R., Zhong,N., Amato,N.J., Liu,Y., Liu,S., Cai,Q., Ji,D., Jin,S.G., Niedernhofer,L.J. *et al.* (2014) Tet-mediated formation of 5-hydroxymethylcytosine in RNA. *J. Am. Chem. Soc.*, **136**, 11582–11585.
66. Delatte,B., Wang,F., Ngoc,L.V., Collignon,E., Bonvin,E., Deplus,R., Calonne,E., Hassabi,B., Putmans,P., Awe,S. *et al.* (2016) RNA biochemistry. Transcriptome-wide distribution and function of RNA hydroxymethylcytosine. *Science*, **351**, 282–285.
67. Sprinzl,M. and Vassilenko,K.S. (2005) Compilation of tRNA sequences and sequences of tRNA genes. *Nucleic Acids Res.*, **33**, D139–D140.